Atmos. Chem. Phys. Discuss., doi:10.5194/acp-2016-246, 2016
Manuscript under review for journal Atmos. Chem. Phys.
Published: 11 April 2016

Atmospheric Chemistry and Physics Discussions

Saharan dust contribution to the Caribbean summertime boundary layer - A lidar study during SALTRACE

Silke Groß[1], Josef Gasteiger[2], Volker Freudenthaler[2], Thomas Müller[4], Daniel Sauer[1], Carlos Toledano[3], and Albert Ansmann[4]

[1]Deutsches Zentrum für Luft- und Raumfahrt, Institut für Physik der Atmosphäre, Münchner Str. 20, 82234 Oberpfaffenhofen, Germany
[2]Ludwig-Maximilians-Universität, Meteorologisches Institut, Theresienstr. 37, 80333 München, Germany
[3]Universitat de Valladolid, Valladolid, Spain.
[4]Leibnitz-Insitut für Troposphärenforschung (TROPOS), Permoserstr. 15, 04318 Leipzig, Germany

Correspondence to: S. Groß (silke.gross@dlr.de)

Abstract. Dual-wavelength lidar measurements with the small lidar system POLIS of the Ludwig-Maximilians-Universität München were performed during the SALTRACE experiment at Barbados in June and July 2013. Based on high accurate measurements of the linear depolarization ratio down to about 150–200 m above ground level, the dust volume fraction and the dust mass concentration within the Caribbean boundary layer can be derived. Additional information from radiosonde launches at the ground-based measurement site provide independent information of the boundary layer height and the meteorological situation within the boundary layer. We investigate the lidar derived optical properties, the lidar ratio and the particle linear depolarization ratio at 355 and 532 nm and find over all mean values and mean uncertainties of 0.04 ± 0.03 and 0.05 ± 0.04 at 355 and 532 nm, respectively, for the particle linear depolarization ratio, and 26 ± 5 sr for the lidar ratio at 355 and 532 nm. For the concentration of dust in the Caribbean boundary layer we find that most values are between 20 and 50 $\mu g/m^3$, and that on most days the dust contribution to total aerosol volume is about 30–40%. Comparing the dust contribution to the column-integrated sun-photometer measurements we see a correlation of high dust contribution, high total aerosol optical depth and a corresponding low Angström exponent, and of low dust contribution with low total aerosol optical depth and corresponding high Angström exponent. The relative humidity within the boundary layer was high with values around 80% on most of the days.

1 Introduction

Saharan dust is one main component of the global aerosol load (Forster and et al., 2007; Haywood and Boucher, 2000) with an estimated annual emission of more than 1000 Mt (Duce et al., 1991). Saharan dust can be transported for several thousand kilometers (Goudie and Middleton, 2001; Liu et al., 2008), influencing the Earth's energy budget on its way (Tegen et al., 1997). Turbulent downward mixing of dust in the marine boundary layer over the tropical Atlantic is assumed to be an efficient dust removal process. To support modeling efforts to accurately simulate dust long-range transport and removal processes, a high-quality vertically resolved characterization of the optical and microphysical particle properties in the marine boundary

Atmos. Chem. Phys. Discuss., doi:10.5194/acp-2016-246, 2016
Manuscript under review for journal Atmos. Chem. Phys.
Published: 11 April 2016

Atmospheric Chemistry and Physics Discussions

layer as well as in the main dust layer (Saharan Air Layer, SAL) is necessary. SAL properties are already presented by Groß et al. (2015). Here, we present the properties for the CMBL (convective marine boundary layer). In this context, it should be mentioned that further papers will be presented that will also partly deal with the removal of dust by turbulent downward mixing in the framework of this SALTRACE special issue (Rittmeister et al., in preparation; Marinou et al., in preparation).

The typically cloud-topped convective boundary layer in the trade-wind-dominated tropics consists of the so-called sub-cloud layer, which is identical with the convective boundary layer in the absence of cloud formation and typically reaches to 500-1000 m height, and the cloud layer (Siebert et al., 2013). Moist convection can lead to a considerable increase of the overall depth of the convectively active height range. Over Barbados, cloud top heights were frequently observed from 1500-2500 m. In the convectively active zone, the observed particle linear depolarization is usually low (< 0.1) and rapidly increases to typical values > 0.2 in the basis of the lofted mineral dust layer (Groß et al. 2015, Haarig et al., in preparation for this special issue). This strong increase at the top of the cloud-topped or cloud-less CMBL is to our opinion a clearly sign for an efficient downward mixing of dust at the interface between the CMBL and the lofted SAL. Dust trapped in the CMBL will then be comparably quickly transported down to the ocean or land surface and deposited.

As shown by Marinou et al. (in preparation for this special issue) in terms of the particle linear depolarization ratio measured by the CALIOP space lidar, the CMBL depth is low close to western Africa in summer and increases with distance from Africa. This finding is in agreement with shipborne lidar observations in May 2013 (Rittmeister et al., in preparation for this special issue). Frequent cloud formation in the marine boundary layer change the thermodynamic conditions in the range from about 700 to 1500-2000 m towards less stable air stratification and more higher moisture levels so that subsequent cloud formation is facilitated and clouds may reach higher altitudes.

In this work we present information of the CMBL and the dust contribution within the CMBL over Barbados in June and July 2013. This information is based on ground-based lidar measurements with the depolarization and Raman lidar system POLIS (Freudenthaler et al., 2015; Groß et al., 2015) of the Ludwig-Maximilians-Universität, München, performed in cooperation with the Deutsches Zentrum für Luft- und Raumfahrt (DLR), and on radiosonde measurements (launched typically twice a day) over the Barbados ground-base site performed from the Leibnitz-Insitut of tropospheric research (TROPOS), Leipzig. The measurements were conducted in the framework of the Saharan Aerosol Long-range Transport and Cloud-interaction Experiment (SALTRACE) in June and July 2013. The measurement site was located at the area of the Caribbean Institute of Meteorology and Hydrology (CIMH) at Husbands (13.14° N, 59.62° W, 100 m), on the south-western part of Barbados.

The general properties discussed in this paper include the height, the wind direction and wind speed of the boundary layer. The lidar derived properties include the mean lidar ratio and mean particle depolarization ratio within the boundary layer at 355 nm and 532 nm, as well as the retrieved dust volume fraction and dust concentration within the boundary layer. The aim of this paper is to provide a detailed boundary layer characterization as part of the vertical aerosol structure over Barbados during SALTRACE. This is important as it enables to link ground-based dust measurements, airborne measurements, and column-integrated measurements e.g. with sun-photometers.

This paper is structured as follows; in Section 2 the measurements, the instrumentation, and the methodology are briefly described, in Section 3 the results are presented, and Section 4 concludes this work.

Atmos. Chem. Phys. Discuss., doi:10.5194/acp-2016-246, 2016
Manuscript under review for journal Atmos. Chem. Phys.
Published: 11 April 2016

Atmospheric Chemistry and Physics Discussions

2 Method

2.1 Aerosol type separation

From the profiles of the particle linear depolarization ratio δ_{p} and particle backscatter coefficient β_{p} measured at 532 nm we determine the dust backscatter coefficient β_{d} following the procedure described by Tesche et al. (2009a); Groß et al. (2011a) and Ansmann et al. (2011). This method is based on the work of Shimizu et al. (2004) assuming a two component mixture with known particle depolarization ratio of the two components. Comparisons with coordinated in-situ measurements justify the assumption of a two component mixture of marine aerosols and mineral dust for this study. It was shown that long-range transported dust does not show enhanced hygroscopicity and that the chemical composition of the dust remaines rather unchanged (Denjean et al., 2015). The relative humidity within the boundary layer was always higher 60% so that we do not consider any dry marine aerosols within the boundary layer (Murayama et al., 1999; Sakai et al., 2010). Thus, we used as input parameters at 532 nm a mean dust linear depolarization ratio δ_{d} of 0.30 (Freudenthaler et al., 2009; Groß et al., 2011b, 2015) and a mean marine (non-dust) linear depolarization ratio δ_{nd} of 0.02 for relative humidity values $\geq$45% (Groß et al., 2011b). The dust α_{d} and marine extinction coefficient α_{nd} are calculated according to $\alpha = \beta \cdot S$ with a mean dust lidar ratio S_{d} of 55 sr (Tesche et al., 2009b; Groß et al., 2015) and a mean marine lidar ratio S_{nd} of 20 sr (Groß et al., 2015) at 532 nm.

2.2 Dust volume and mass conversion

In a next step the volume concentration of both particle types is derived using a conversion factor from extinction to volume concentration v/α. This conversion factor strongly depends on the microphysical properties of the aerosol type, in particular on the size distribution, and the refractive index. The conversion factor v/α of the reference ensemble of Gasteiger et al. (2011) is $0.68{\cdot}10^{-6}$ m for a wavelength of 532nm. This ensemble was found to be consistent with lidar measurements of Saharan aerosol in Morocco during SAMUM-1. To study the potential differences in the conversion factor v/α for fresh and long-range transported dust, v/α was also derived from SAMUM-1 and SALTRACE-AERONET measurements during pure dust periods, showing a constant value of v/α=$0.65{\cdot}10^{-6}$ m (not shown here). Thus we use a dust conversion factor of v/α=$0.65{\cdot}10^{-6}$ m in this study. To derive the conversion factor for marine aerosols AERONET measurements at Barbados from 2007–2015 were analyzed, resulting in a conversion factor v/α=$0.66{\cdot}10^{-6}$ m. The dust volume fraction can then easily be calculated from the ratio of the dust volume concentration to the total volume concentration. The dust mass concentration is calculated from the dust volume concentration by multiplication with the particle density, which we assumed to be 2.5 g/cm^{-3} according to mixtures of coarse and fine mode particles (Ansmann et al., 2011; Mamouri and Ansmann, 2014) and sulfate particles (Kaaden et al., 2009).

2.3 CMBL height identification

From the radiosonde measurements we inferred the height of the CBL. As turbulent convection in the boundary layer causes constant values of the potential temperature and mixing ratio (Hooper and Eloranta, 1986; Kaimal et al., 1976), we use these

Atmos. Chem. Phys. Discuss., doi:10.5194/acp-2016-246, 2016
Manuscript under review for journal Atmos. Chem. Phys.
Published: 11 April 2016

Atmospheric Chemistry and Physics Discussions

properties as indicators for the CMBL height. Furthermore we used temperature information derived from the radiosonde ascents, as the boundary layer is mostly capped by an inversion layer (Carson, 1973). Independently we derived the CMBL height from the optical properties measured with our lidar system. Aerosol concentration and thus the aerosol backscatter coefficient show a gradient on top of the boundary layer (Boers et al., 1984; Hooper and Eloranta, 1986) which we used to determine the CMBL height.

3 Results

3.1 General measurement situation

The main measurement period for closure studies during SALTRACE was from 20 June to 12 July 2013. During this time the aerosol situation above Barbados was characterized by an aerosol optical depth (AOD) which mainly ranged between about 0.2 and 0.4 nearly wavelength-independent for the CIMEL measurements at 340, 500 and 1020 nm (Fig. 1). The Angström Exponent (AE) was typically 0.2 or lower. On some days, however, the aerosol load over Barbados was very low, with AOD values below 0.2. Those low AOD values were connected with higher AE of about 0.5–0.7. On 7 July 2013 the AE was even as high as 1.1. Five episodes with AOD values higher (up to 0.6) were observed.

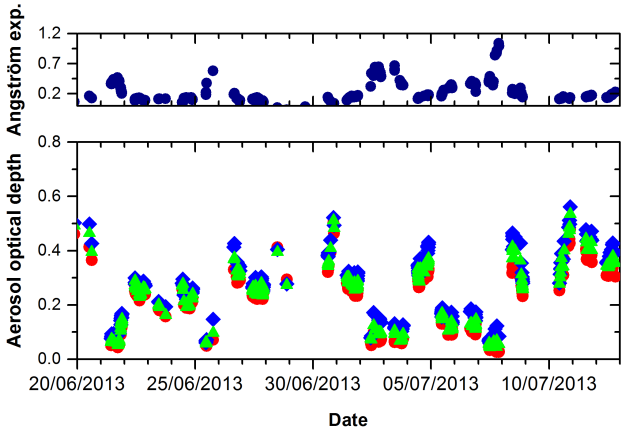

Figure 1. Shown is the Angström Exponent between 440 and 870 nm (upper panel) and the Aerosol optical depth at 340 (blue), 500 (green) and 1020 nm (red) derived from AERONET-CIMEL sun-photometer measurements at the Caribbean Institute for Meteorology and Hydrology, Barbados (data: Barbados_SALTRACE) from 20 June to 13 July 2013

3.2 Case study – 10 July 2013

A multi-layer aerosol structure was observed over Barbados during SALTRACE in June and July 2013. Figure 2 provides an overview of the situation on 10 July 2013 based on aerosol lidar observation at 532 nm with POLIS. The general structure of the shown profiles is representative for most of the SALTRACE measurements (Groß et al., 2015). From the volume and

Atmos. Chem. Phys. Discuss., doi:10.5194/acp-2016-246, 2016
Manuscript under review for journal Atmos. Chem. Phys.
Published: 11 April 2016

Atmospheric Chemistry and Physics Discussions

particle linear depolarization ratio (Fig. 2b) two aerosol regimes are clearly identified; in the lowermost 1.5 km the particle depolarization ratio is around or even below 0.1, which is an indication that dust has only a minor contribution to the aerosol mixture. Above about 1.6 km the volume and particle linear depolarization ratio is clearly higher with values of about 0.14 to 0.18 for the volume linear depolarization ratio and 0.28 to 0.3 for the particle linear depolarization ratio. The separation of the two aerosol regimes is also visible in the radiosonde measurements started at 17:49 UTC (Fig. 2e,f) showing a temperature inversion between about 1.6 and 1.8 km height together with a change in relative humidity, mixing ratio, potential temperature and wind speed (not shown).

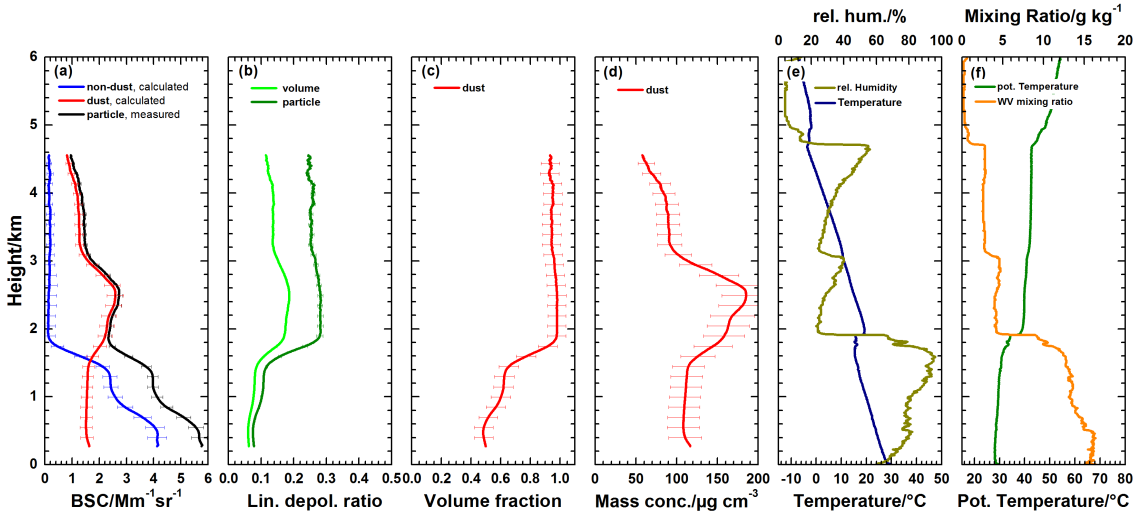

Figure 2. Shown is (a) the separation of dust (red) and non-dust (blue) particle backscatter coefficient (BSC) at 532 nm from total particle backscatter coefficent (black) at 532 nm, (b) measured volume (light green) and particle (dark green) linear depolarization ratio at 532 nm, (c) dust volume fraction, (d) dust concentration derived from POLIS measurements at Barbados on 10 July 2013 at 20 UTC, (e) temperature (dark blue) and relative humidity (dark yellow) profiles, and (f) profiles of potential temperature (dark green) and water vapor mixing ratio (orange) derived from radiosonde measurements started on 10 July 2013 at 17:49 UTC. Error bars give the systematical uncertainties resulting from measurement uncertainties and uncertainties in the lidar specific input parameters.

According to the criteria for CMBL height identification with lidar (Boers et al., 1984; Hooper and Eloranta, 1986) the CMBL height on 10 July 2013 is at about 500 m. Lidar measurements show a strong gradient in the aerosol backscatter coefficient (Fig. 2a) at about 500 m. CMBL height detection from radiosonde measurements at 17:49 UTC is not that distinctive; only the water vapor mixing ratio shows slight changes. The capping inversion in the temperature profile and the change in the potential temperature on top of the CMBL are missing or not pronounced. Also the measured volume and particle linear depolarization ratio (Fig. 2b) within the CMBL show only slight differences compared to the values found in the transition layer between the CMBL and the Saharan air layer. The CMBL is characterized by a constant value of the potential temperature of about 28°C and a constant water vapor mixing ratio of about 16 g/kg. The relative humidity within the boundary layer increases with height from about 65 to 80%. The wind in the boundary layer (not shown) comes from easterly directions with

Atmos. Chem. Phys. Discuss., doi:10.5194/acp-2016-246, 2016
Manuscript under review for journal Atmos. Chem. Phys.
Published: 11 April 2016

Atmospheric Chemistry and Physics Discussions

a mean wind speed around 7 m/s. The aerosol optical depth within the boundary layer is about 0.1 at 532 nm (not shown) and the mean volume and particle depolarization ratio at 532 nm are about 0.06 and 0.08, respectively.

Following the procedure described in Section 2.2 the volume fraction of dust is derived (Fig. 2c). Above about 1.6 km dust contributes to about 100 % to the total aerosol volume while below 1.5 km height the dust contribution is only 70 % or less. In the boundary layer (lowermost 0.5 km) the dust volume fraction is even less than 60 %. For the dust concentration (Fig. 2d) we find a rather constant value of about 0.11 μg/cm in the lowest 1.5 km. Above 1.5 km height the profile of the dust concentration follows in general the profile of the backscatter coefficient (Fig. 2a) with a maximum in dust concentration of about 190 $\mu g/cm^3$ between 1.4 and 1.6 km height.

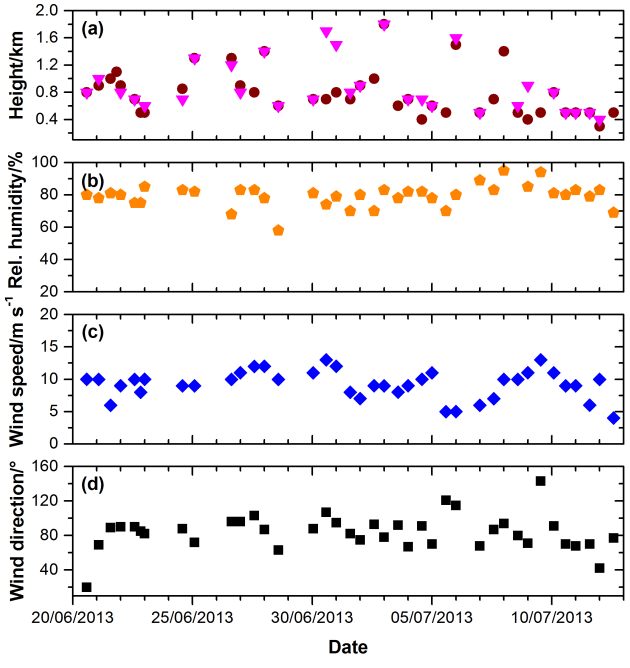

Figure 3. Shown is (a) the CMBL height derived from radiosonde measurements (brown dots) and lidar measurements (magenta rectangles), (b) the mean relative humidity within the CMBL derived from radiosonde measurements, (c) the mean wind speed in the CMBL measured with radiosonde, and (d) the mean wind direction in the CMBL derived from radiosonde measurements.

3.3 CMBL height and conditions

As described in Section 2.3 the CMBL height is derived from radiosonde and lidar measurements (Fig. 3a). The CMBL top above our measurement site during SALTRACE is mainly between 0.5 and 0.9 km, in some cases the boundary layer top is even higher up to 1.8 km. The CMBL height derived from radiosondes and lidar mostly agree within 100 m, however in a few cases the CMBL height derived from lidar measurements is higher than the CMBL height derived from radiosondes. In these cases the CMBL height from radiosondes is mainly derived from changes in the mixing ratio. In all these cases we do not see

Atmos. Chem. Phys. Discuss., doi:10.5194/acp-2016-246, 2016
Manuscript under review for journal Atmos. Chem. Phys.
Published: 11 April 2016

Atmospheric Chemistry and Physics Discussions

a profound change in the potential temperature nor a capping inversion layer on top of the CMBL. A pronounced temperature inversion and change in the potential temperature at these cases is found in height ranges of the lidar derived CMBL heights. We frequently found, that pronounced changes of the intensive lidar quantities on top the CMBL are often connected with strong capping inversions and changes in potential temperature on top of the CMBL, while the differences of the intensive optical properties between CMBL and transition layer was not pronounced in cases when capping inversion on top the CMBL was missing and changes in potential temperature were only little. Those cases mainly occurred during the daytime measurements.

During SALTRACE the relative humidity within the boundary layer is quite high with values around 80%. Only on a few days the relative humidity within the boundary layer is lower, but the values are never lower than 60% (Fig. 3b). The mean wind speed within the boundary layer over Barbados during SALTRACE is mainly between 8 and 12 $\mathrm{m/s}$ (Fig. 3c), and therewith represents optimal conditions for the production of sea salt particles (Gong, 2003; Knippertz et al., 2011). Between 5 July and 7 July 2013 as well as during individual days between 20 June and 23 June 2013 the wind speed is lower with values around 6 $\mathrm{m/s}$, but these values are still higher than the empirically derived threshold for sea-salt production of 5.5 $\mathrm{m/s}$ (Knippertz et al., 2011). Only on the last days of our measurements the wind speed is lower than this empirical value.

From our measurements we assume, that sea salt particles can only be detected below about 1500 m at Barbados, most likely advected to our measurement site by strong onshore easterly winds. The wind direction within the CMBL derived from radiosondes (Fig. 3d) is mainly East to North-East, except for very few cases when the wind flows from either northern or southern directions.

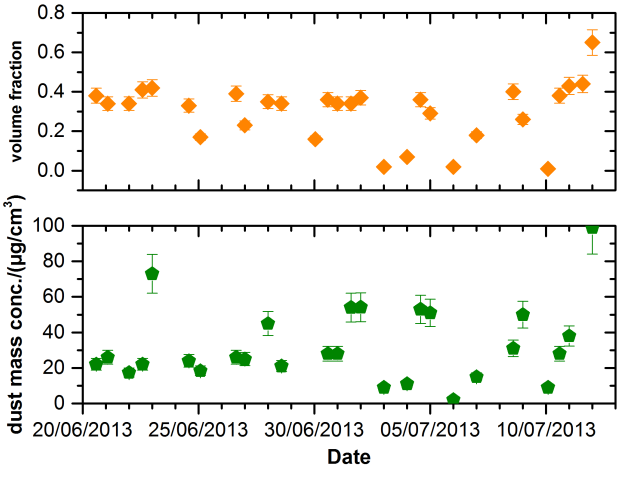

Figure 4. Shown is the dust volume fraction (upper panel) and the dust mass concentration (lower panel) within the CMBL over Barbados derived from POLIS lidar measurements. Error bars give the systematical uncertainties resulting from measurement uncertainties and uncertainties in the lidar specific input parameters.

Atmos. Chem. Phys. Discuss., doi:10.5194/acp-2016-246, 2016
Manuscript under review for journal Atmos. Chem. Phys.
Published: 11 April 2016

Atmospheric Chemistry and Physics Discussions

3.4 Dust contribution in the CMBL

Figure 4 shows the mean dust volume fraction and the mean dust mass concentration within the CMBL retrieved from our lidar measurements. The dust volume fraction within the CMBL shows values between 0.01 and 0.65. The majority of days show values between about 0.3 and about 0.4. The dust mass concentration within the CMBL ranges between 2 and 100 $\mu g/cm^3$ with most frequent values between 20 and 50 $\mu g/cm^3$. Comparing the dust volume fraction and dust mass concentration within the CMBL with total AOD at 500 nm and AE (between 440 and 870 nm) for the complete atmospheric column derived from sun-photometer measurements (Fig. 1) , one can see that days with low dust volume fraction and low dust mass concentration within the CMBL are found for days with column integrated AOD ≤ 0.1 at 500 nm and corresponding AE ≥ 0.4. The highest values of the dust volume fraction and the dust mass concentration are found for days with high AOD ≥ 0.4 nm and corresponding low AE of ≤ 0.2.

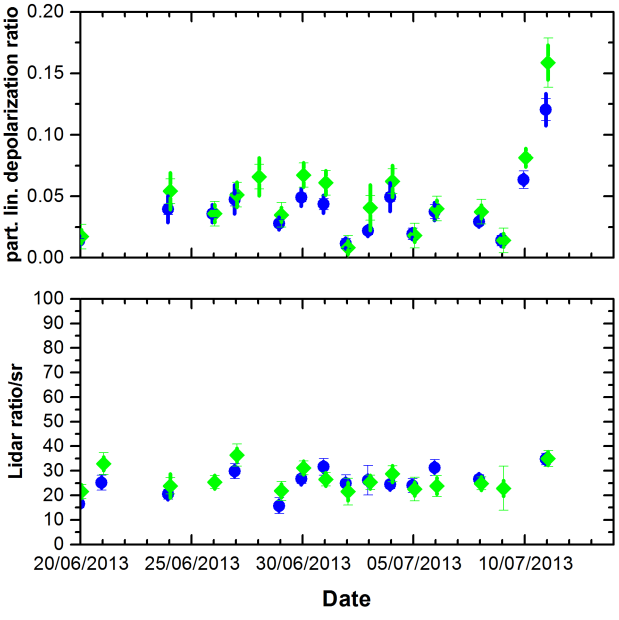

Figure 5. Shown are the mean values of the particle linear depolarization ratio (upper panel) and the lidar ratio (lower panel) at 355 and 532 nm measured with POLIS within the boundary layer. The thick lines show the standard deviation of the mean, the thin error bars denote the mean systematic errors.

3.5 Optical properties within the CMBL

Except for the last dust event during the SALTRACE campaign, the CMBL during SALTRACE is characterized by low values of the particle linear depolarization ratio and the lidar ratio ranging between 0.01–0.08 and 15–31 sr at 355 and 532 nm (Fig. 5). These values are in good agreement with the findings of Murayama et al. (1999), who found mean values of the particle

Atmos. Chem. Phys. Discuss., doi:10.5194/acp-2016-246, 2016
Manuscript under review for journal Atmos. Chem. Phys.
Published: 11 April 2016

Atmospheric Chemistry and Physics Discussions

Table 1. Mean values of the lidar ratio and particle linear depolarization ratio (PLDR) including the mean systematic errors (±) for different aerosol types and their dominant time periods.

Dominant type	Date	PLDR		Lidar ratio/sr	
		355 nm	532 nm	355 nm	532 nm
marine	20, 29 June 2, 5, 9 July	0.02 ± 0.01	0.02 ± 0.01	20 ± 3	22 ± 5
dust and marine (marine-dominated)	24 June - 10 July without marine cases	0.04 ± 0.01	0.05 ± 0.01	27 ± 3	28 ± 3
dust and marine (dust-dominated)	11 July	0.12 ± 0.01	0.15 ± 0.02	35 ± 3	35 ± 3
overall		0.04 ± 0.03	0.05 ± 0.04	26 ± 5	26 ± 5

linear depolarization ratio at 532 nm of 0.01 and 0.1 in a dust influenced marine boundary layer. They related the lower values to pure marine aerosols whereas they assumed a contribution of dust for the higher values. Similar to Murayama et al. (1999) and Groß et al. (2011b, a) we assign values of the particle linear depolarization ratio of 0.01–0.03 (mean value 0.02) at 355 and 532 nm to marine aerosols, which is in good agreement with the findings of Sakai et al. (2010), who found values of 0.01 for sea-salt droplets from laboratory chamber measurements at 532 nm. The corresponding values of the lidar ratio for the marine aerosol cases are 16–24 sr with mean values of 20 ± 3 at 355 nm and of 22 ± 5 at 532 nm. These values are also in good agreement to former findings from theoretical studies (Ackermann, 1998) and measurements (Groß et al., 2011b, a). During the last measurement day the mean value of the lidar ratio within the CMBL is about 35 sr wavelength independent, and the particle linear depolarization ratio shows mean values of about 0.12 at 355 nm and of about 0.16 at 532 nm, indicating a larger amount of mineral dust (Murayama et al., 1999; Groß et al., 2011b). The overall values of the particle linear depolarization ratio are wavelength independent with mean values of 0.04 ± 0.03 at 355 nm and 0.05 ± 0.04 at 532 nm. The overall mean value of the lidar ratio within the boundary layer is 26 ± 5 sr at 355 and 532 nm.

According to former findings (e.g. Ackermann 1998; Sakai et al. 2010; Murayama et al. 1999; Groß et al. 2011b, a) and lidar based aerosol classification schemes (Groß et al., 2011b; Burton et al., 2012; Groß et al., 2013) we find four days during the whole SALTRACE measurement period with a pure marine boundary layer, one day with dust dominated dust-marine mixture within the CMBL, and on all the other days we assign the marine-dominated mixture within the CMBL. The results of the optical properties within the CMBL during SALTRACE are summarized in Table 1.

Atmos. Chem. Phys. Discuss., doi:10.5194/acp-2016-246, 2016
Manuscript under review for journal Atmos. Chem. Phys.
Published: 11 April 2016

Atmospheric Chemistry and Physics Discussions

3.6 Closure

To validate the lidar derived dust contribution (i.e. dust volume fraction and dust mass concentration), we compared the lidar derived dust mass concentration with synchronized ground-based in-situ measurements of dust concentration at Ragged Point (Kristensen et al. 2016; Müller et al., in preparation for this special issue) at the eastern coast of Barbados (Fig. 6). The ambient aerosol was sampled through a PM10 inlet (i.e. nominal cut-off at r=5μm) for the in-situ measurements (Kristensen et al., 2016). Thus a certain fraction of the ambient dust mass possibly is not covered by the in-situ measurements. Using the OPAC desert mixture and assuming that particles up to r=10μm reach the Barbados measurement site, we deduced that the mass concentration derived from the in-situ measurements needs to be multiplied by a factor of about 1.25 to get ambient mass concentration. However, as the coarse mode size distribution of transported dust is not well characterized, we assume an uncertainty of $\pm$0.25 for that factor. The factor 1.25 $\pm$ 0.25 is considered in Fig. 6.

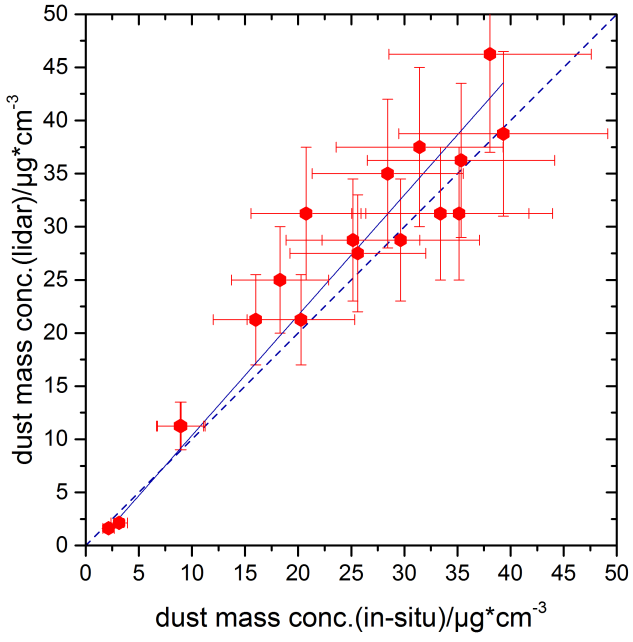

Figure 6. Shown is the dust dust mass concentration derived from lidar analysis versus the dust mass concentration measured in-situ at Ragged Point. Only measurements that match in time are plotted. Error bars for the lidar derived dust mass concentration give the systematic uncertainties resulting from measurement uncertainties and lidar specific input parameters. Error bars for the in-situ derived dust mass concentration result from the nominal cut-off and the assumed dust mass which thus can not be covered by the in-situ measurements. The straight line gives the linear fit of all measurement points, the dashed line the one-to-one line.

The dust concentration derived from both methods shows in general a very good agreement. The mean difference between both methods is about 3 $\mu g/cm^3$. A linear fit considering all synchronized measurements has a slope of 1.1 with a tendency for larger values of the lidar derived dust mass concentration at higher dust mass concentration in the CMBL. The mean lidar

Atmos. Chem. Phys. Discuss., doi:10.5194/acp-2016-246, 2016
Manuscript under review for journal Atmos. Chem. Phys.
Published: 11 April 2016

Atmospheric Chemistry and Physics Discussions

and mean in-situ derived dust mass concentration do not show systematic differences considering the uncertainties of both methods.

4 Summary

We used ground-based lidar measurements and radiosonde data to study the boundary layer over Barbados and to derive the dust contribution. Therefore we applied a well described method for aerosol type separation presented by Tesche et al. (2009a) and (Groß et al., 2011a). We found good agreement between the boundary layer height derived from radiosonde data and lidar measurements. The boundary layer height was about 0.4 to 1.8 km. The optical properties in the boundary layer were mainly dominated by marine aerosols with mean linear particle depolarization ratios of 0.01—0.08 at 355 and 532 nm and mean lidar ratios of 15–31 sr at both wavelengths. The volume fraction of dust within the boundary layer was mainly between 0.3 and 0.4 except on days with low aerosol load. The corresponding dust concentration on most days was 20 and 50 $\mu g/cm^3$. We found a very good agreement between our lidar derived dust concentration and in-situ measurements performed on the eastern part of the island.

Acknowledgements. The SALTRACE campaign was mainly funded by the Helmholtz Association, the Deutsches Zentrum für Luft- und Raumfahrt (DLR), the Ludwig-Maximilians-Universität München (LMU) and the Institut für Troposphärenforschung (TROPOS). This work project was partly founded by a DLR VO-R young investigator group, by the Deutsche Forschungsgemeinschaft (DFG) in the SPP (no. 1294/2) "Atmosphären- und Erdsystemforschung mit dem Forschungsflugzeug HALO" under contract no. KI1567/1-1, and the LMU Munichs Institutional Strategy LMUexcellent within the framework of the German Excellence Initiative. The lidar and sun-photometer measurements were performed at the site of the Caribbean Institute for Meteorology and Hydrology (CIMH). We thank CIMH for providing us with this measurement environment.

Atmos. Chem. Phys. Discuss., doi:10.5194/acp-2016-246, 2016
Manuscript under review for journal Atmos. Chem. Phys.
Published: 11 April 2016

Atmospheric Chemistry and Physics Discussions

References

Ackermann, J.: The Extinction-to-Backscatter Ratio of Tropospheric Aerosol: A Numerical Study, Journal of Atmospheric and Oceanic Technology, 15, 1043–1050, doi:10.1175/1520-0426(1998)015<1043:TETBRO>2.0.CO;2, http://journals.ametsoc.org/doi/abs/10.1175/1520-0426%281998%29015%3C1043%3ATETBRO%3E2.0.CO%3B2, 1998.

Ansmann, A., Petzold, A., Kandler, K., Tegen, I., Manfred, W., Müller, D., Weinzierl, B., Müller, T., and Heintzenberg, J.: Saharan Mineral Dust Experiments SAMUM-1 and SAMUM-2: what have we learned?, Tellus B, 63, 403–429, doi:10.1111/j.1600-0889.2011.00555.x, http://dx.doi.org/10.1111/j.1600-0889.2011.00555.x, 2011.

Boers, R., Eloranta, E. W., and Coulter, R. L.: Lidar Observations of Mixed Layer Dynamics: Tests of Parameterized Entrainment Models of Mixed Layer Growth Rate, J. Climate Appl. Meteor., 23, 247–266, doi:http://dx.doi.org/10.1175/1520-0450(1984)023<0247:LOOMLD>2.0.CO;2, 1984.

Burton, S. P., Ferrare, R. A., Hostetler, C. A., Hair, J. W., Rogers, R. R., Obland, M. D., Butler, C. F., Cook, A. L., Harper, D. B., and Froyd, K. D.: Aerosol classification using airborne High Spectral Resolution Lidar measurements - methodology and examples, Atmospheric Measurement Techniques, 5, 73–98, doi:10.5194/amt-5-73-2012, http://www.atmos-meas-tech.net/5/73/2012/, 2012.

Carson, D. J.: The development of a dry inversion-capped convectively unstable boundary layer, Quarterly Journal of the Royal Meteorological Society, 99, 450–467, doi:10.1002/qj.49709942105, http://dx.doi.org/10.1002/qj.49709942105, 1973.

Denjean, C., Caquineau, S., Desboeufs, K., Laurent, B., Maille, M., Quiñones Rosado, M., Vallejo, P., Mayol-Bracero, O. L., and Formenti, P.: Long-range transport across the Atlantic in summertime does not enhance the hygroscopicity of African mineral dust, Geophysical Research Letters, pp. n/a–n/a, doi:10.1002/2015GL065693, http://dx.doi.org/10.1002/2015GL065693, 2015GL065693, 2015.

Duce, R., Liss, P., Merrill, J., Atlas, E., Buat-Menard, P., Hicks, B., Miller, J., Prospero, J., Arimoto, R., Church, T., et al.: The atmospheric input of trace species to the world ocean, Global biogeochemical cycles, 5, 193–259, 1991.

Forster, P. and et al.: Changes in atmospheric constituents and in radiative forcing, Climate Change 2007: The Physical Science Basis. Contribution of Working Group I to the Fourth Assessment Report of the Intergovernmental Panel on Climate Change, Cambridge University Press, pp. 210–215, 2007.

Freudenthaler, V., Esselborn, M., Wiegner, M., Heese, B., Tesche, M., Ansmann, A., Müller, D., Althause, D., Wirth, M., Fix, A., Ehret, G., Knippertz, P., Toledano, C., Gasteiger, J., Garhammer, M., and Seefeldner, M.: Depolarization ratio profiling at several wavelengths in pure Saharan dust during SAMUM 2006., Tellus B, 61, 165–179, 2009.

Freudenthaler, V., Seefeldner, M., Groß, S., and Wandinger, U.: Accuracy of linear depolarisation ratios in clean air ranges measured with POLIS-6 at 355 and 532 nm., Proceeding of 27. International Laser Radar Conference, New York, 2015.

Gasteiger, J., Wiegner, M., Groß, S., Freudenthaler, V. Toledano, C., Tesche, M., and Kandler, K.: Modeling lidar-relevant optical properties of complex mineral dust aerosols, Tellus B, 63, 2011.

Gong, S. L.: A parameterization of sea-salt aerosol source function for sub- and super-micron particles, Global Biogeochemical Cycles, 17, n/a–n/a, doi:10.1029/2003GB002079, http://dx.doi.org/10.1029/2003GB002079, 1097, 2003.

Goudie, A. and Middleton, N.: Saharan dust storms: nature and consequences., Earth-Science Reviews, 56, 179–204, 2001.

Groß, Freudenthaler, V., Wirth, M., and Weinzierl, B.: Towards an aerosol classification scheme for future EarthCARE lidar observations and implications for research needs, Atmospheric Science Letters, 16, 77–82, doi:10.1002/asl2.524, http://dx.doi.org/10.1002/asl2.524, 2015.

Groß, S., Gasteiger, J., Freudenthaler, V., Wiegner, M., Geiß, A., Toledano, C., Kandler, K., Tesche, M., Ansmann, A., and Wiedensohler, A.: Characterization of the planetary boundary layer during SAMUM-2 by means of lidar measurements, Tellus, B 63, 695–705, 2011a.

Groß, S., Tesche, M., Freudenthaler, V., Toledano, C., Wiegner, M., Ansmann, A., Althausen, D., and Seefeldner, M.: Characterization of Saharan dust, marine aerosols and mixtures of biomass burning aerosols and dust by means of multi-wavelength depolarization- and Raman-measurments during SAMUM-2, Tellus B, 63, 706 – 724, doi:10.1111/j.1600-0889.2011.00556.x, tellus B63, 2011b.

Groß, S., Esselborn, M., Weinzierl, B., Wirth, M., Fix, A., and Petzold, A.: Aerosol classification by airborne high spectral resolution lidar observations, Atmospheric Chemistry and Physics, 13, 2487–2505, doi:10.5194/acp-13-2487-2013, http://www.atmos-chem-phys.net/13/2487/2013/, 2013.

Haywood, J. and Boucher, O.: Estimates of the direct and indirect radiative forcing due to tropospheric aerosols: a review., Rev. of Geophysics, 38, 513–543, 2000.

Hooper, W. P. and Eloranta, E. W.: Scanning 6-wavelength 11-channel aerosol lidar, . Climate Appl. Meteor., 25, 990–1001, doi:http://dx.doi.org/10.1175/1520-0450(1986)025<0990:LMOWIT>2.0.CO;2, 1986.

Kaaden, N., Massling, A., Schladitz, A., Müller, T., Kandler, K., Schütz, L., Weinzierl, B., Petzold, A., Tesche, M., Leinert, S., Deutscher, C., Ebert, M., Weinbruch, S., and Wiedensohler, A.: State of mixing, shape factor, number size distribution, and hygroscopic growth of the Saharan anthropogenic and mineral dust aerosol at Tinfou, Morocco, Tellus, B61, 5163, tellus B, 2009.

Kaimal, J. C., Wyngaard, J. C., Haugen, D. A., Cot. R., Izumi, Y., Caughey, S. J., and Readings, C. J.: Turbulence Structure in the Convective Boundary Layer, Journal of Atmospheric Science, 33, 22 152–2169, doi:http://dx.doi.org/10.1175/1520-0469(1976)033<2152:TSITCB>2.0.CO;2, 1976.

Knippertz, P., Tesche, M., Heinold, B., Kandler, K., Toledano, C., and Esselborn, M.: Dust Mobilization and Transport from West Africa to Cape Verde - A Meteorological Overview of SAMUM-2, Tellus, B 63, tellus B, 2011.

Kristensen, T. B., Müller, T., Kandler, K., Benker, N., Hartmann, M., Prospero, J. M., Wiedensohler, A., and Stratmann, F.: Properties of cloud condensation nuclei (CCN) in the trade wind marine boundary layer of the western North Atlantic, Atmospheric Chemistry and Physics, 16, 2675–2688, doi:10.5194/acp-16-2675-2016, http://www.atmos-chem-phys.net/16/2675/2016/, 2016.

Liu, Z., Omar, A., Vaughan, M., Hair, J., Kittaka, C., Hu, Y., Powell, K., Trepte, C., Winker, D., Hostetler, C., Ferrare, R., and Pierce, R.: Calipso lidar observations of the optical properties of saharan dust: A case study of long-range transport, Journal of Geophysical Research, 113, D07 207+, 2008.

Mamouri, R. E. and Ansmann, A.: Fine and coarse dust separation with polarization lidar, Atmospheric Measurement Techniques, 7, 3717–3735, doi:10.5194/amt-7-3717-2014, http://www.atmos-meas-tech.net/7/3717/2014/, 2014.

Murayama, T., Okamoto, H., Kaneyasu, N., Kamataki, H., and Miura, K.: Application of lidar depolarization measurement in the atmospheric boundary layer: Effects of dust and sea-salt particles, Journal of Geophysical Research, 104, 31,78131,792, 1999.

Sakai, T., Nagai, T., Zaizen, Y., and Mano, Y.: Backscattering linear depolarization ratio measurements of mineral, sea-salt, and ammonium sulfate particles simulated in a laboratory chamber, Applied Optics, 49, 4441–4449, doi:10.1364/AO.49.004441, http://ao.osa.org/abstract.cfm?URI=ao-49-23-4441, 2010.

Shimizu, A., Sugimoto, N., Matsui, I., Arao, K., Uno, I., Murayama, T., Kagawa, N., Aoki, K., Uchiyama, A., and Yamazaki, A.: Continuous observations of Asian dust and other aerosols by polarization lidar in China and Japan during ACE-Asia, Journal of Geophysical Research, 109, D19S17, doi:10.1029/2002JD003253, 2004.

Siebert, H., Beals, M., Bethke, J., Bierwirth, E., Conrath, T., Dieckmann, K., Ditas, F., Ehrlich, A., Farrell, D., Hartmann, S., Izaguirre, M. A., Katzwinkel, J., Nuijens, L., Roberts, G., Schäfer, M., Shaw, R. A., Schmeissner, T., Serikov, I., Stevens, B., Stratmann, F., Wehner, B., Wendisch, M., Werner, F., and Wex, H.: The fine-scale structure of the trade wind cumuli over Barbados ndash;

an introduction to the CARRIBA project, Atmospheric Chemistry and Physics, 13, 10 061–10 077, doi:10.5194/acp-13-10061-2013, http://www.atmos-chem-phys.net/13/10061/2013/, 2013.

Tegen, I., Hollrig, P., Chin, M., Fung, I., Jacob, D., and Penner, J.: Contribution of different aerosol species to the global aerosol extinction optical thickness: Estimates from model results, Journal of Geophysical Research, 102, 23,89523,915, 1997.

Tesche, M., Ansmann, A., Müller, D., Althausen, D., Engelmann, R., Freudenthaler, V., and Groß, S.: Vertically resolved separation of dust and smoke over Cape Verde using multiwavelength Raman and polarization lidars during Saharan Mineral Dust Experiment 2008, Journal of Geophysical Research, 114, D13 202, 2009a.

Tesche, M., Ansmann, A., Müller, D., Althausen, D., Mattis, I., Heese, B., Freudenthaler, V., Wiegner, M., Esselborn, M., Pisani, G., and Knippertz, P.: Vertical profiling of Saharan dust with Raman lidars and airborne HSRL in southern Morocco during SAMUM, Tellus, B 61, 144–164, 2009b.